Earth Systems and Environment
https://doi.org/10.1007/s41748-025-00663-6

ORIGINAL ARTICLE

Soil Bulk Density Estimation by a Novel Pedotransfer Function Tailored on Hilly Terrains

Owais Bashir[1] · Shabir Ahmad Bangroo[1] · Sheikh Amjid[1] · Paolo Nasta[2] · Shahid Shafai[1] · Mario Palladino[2] · Nicola Senesi[3] · Rehana Rasool[1] · Burhan U. Choudhury[4] · Prakash Kumar Jha[5] · Vikas Abrol[6] · Velibor Spalevic[7] · Paul Sestras[8,9] · Negar Omidvar[10] · Sezai Ercişli[11] · Lizny Jaufer[12] · Brahim Benzougagh[13] · Youssef Bammou[14] · Ksibi Mohamed[15] · Tin Lukić[16] · Shuraik Kader[17]

Received: 17 November 2024 / Revised: 25 April 2025 / Accepted: 15 May 2025
© The Author(s) 2025

Abstract

The evaluation of soil bulk density (BD) is essential for studying soil processes like water retention, air circulation, and carbon sequestration. Conventional direct BD measurement methods are often time-consuming, costly, and laborious. In contrast, the use of pedotransfer functions (PTFs) based on readily available soil properties offers a cost-effective alternative approach that can provide indirect quick estimates of soil BD. Although several region-specific PTFs are available, none is tailored for use in the hilly North-Western Himalayas (NWH) area. Thus, this work developed a novel PTF to estimate the soil BD of 300 soil samples collected from the NWH area and analyzed by stepwise regression (SR), partial least-squares regression (PLSR), multiple linear regression (MLR), linear regression (LR), and advanced machine-learning algorithms, including artificial neural networks (ANN) and decision tree (DT). The site-specific SR-based equation performed better than the PLSR model by explaining up to 72.2% variability of BD and achieving a coefficient of determination (R^2) of 0.73, a mean absolute error (MAE) of 0.0379 g cm^{-3}, and a root mean square error (RMSE) of 0.0487 g cm^{-3} for the BD prediction. Soil organic matter and clay contents were the most significant contributors, showing the highest importance in the projection. Furthermore, the performance of the SR-based PTF was validated by comparison with 63 PTFs currently in use, which showed to perform poorly and vary widely in BD estimation (R^2: 0.006–0.71, RMSE: 0.0649–0.405 gcm^{-3}, MAE: 0.0512–0.395 g cm^{-3}). The promising SR equation and PTF developed in this work showed high accuracy and excellent suitability for stakeholders and professionals in the study area and the scientific community as a reliable BD estimator for hilly soils. This study introduces proposed the first-ever site-specific PTF for BD estimation in hilly soils, contributing to scientific challenge by enhancing soil database and improving BD predictions in complex terrains worldwide. In terms of global significance, the outcomes of this study are essential for soil quality and vulnerability studies, resilience indicators estimates carbon sequestration initiatives, and digital soil mapping, and can also be used to construct a BD database for hilly soils across the globe.

✉ Shuraik Kader
s.mohamedabdulkader@griffith.edu.au

Extended author information available on the last page of the article

Published online: 23 June 2025

Graphical Abstract

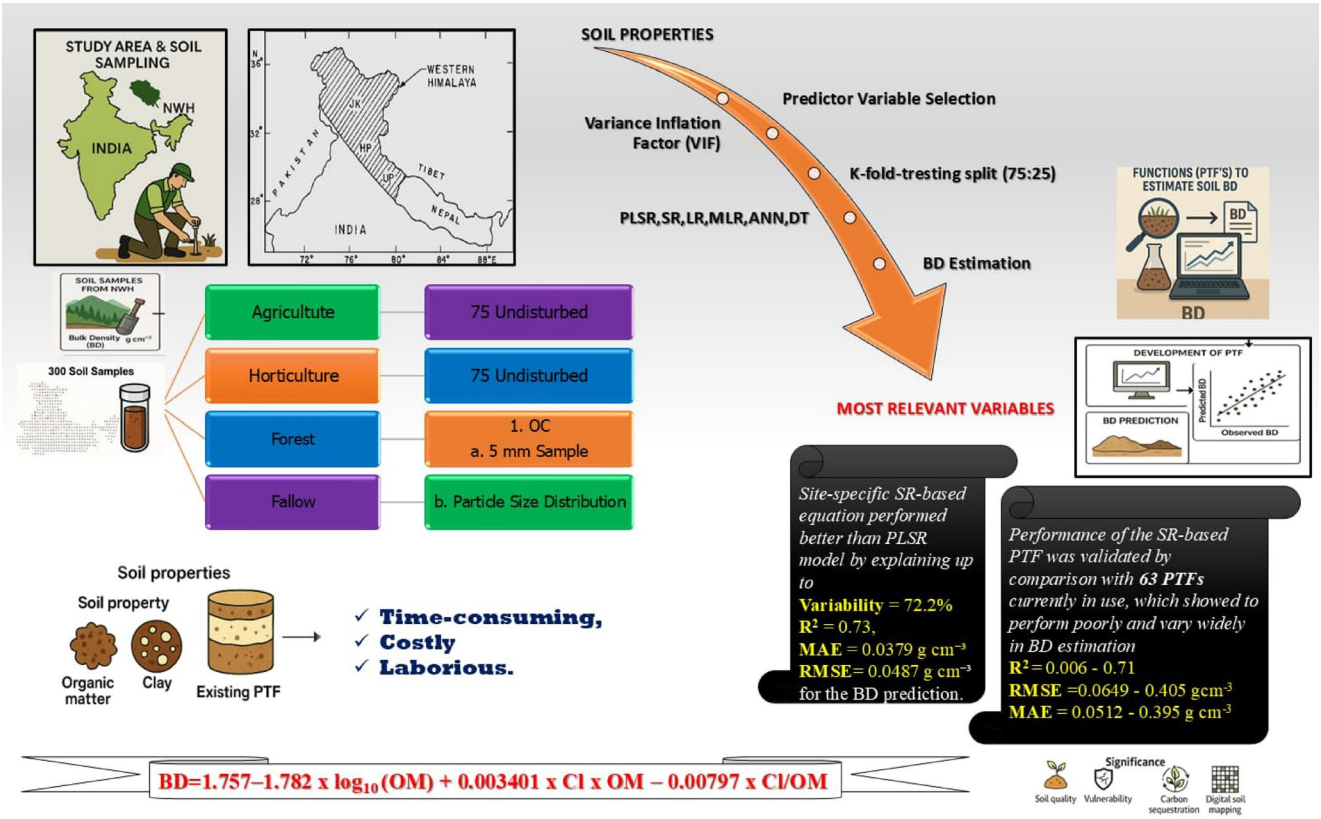

The evaluation of soil bulk density (BD) is essential for studying soil processes like water retention, air circulation and carbon sequestration, and soil quality, vulnerability and resilience. Conventional direct methods to measure soil BD are often time-consuming, costly and laborious, whereas pedotransfer functions (PTFs) based on readily available soil properties offer an efficient alternative approach that provides indirect quick estimates of soil BD. However, none of the several region-specific PTFs currently available, is tailored for use in the hilly North-Western Himalayas (NWH) area. A novel PTF was developed in this work to evaluate the BD of 300 soil samples collected from agriculture, horticulture, forest and fallow hilly soils in the North West Himalaya area. Stepwise regression (SR), partial least-squares regression (PLSR), multiple linear regression (MLR), linear regression (LR), and advanced machine-learning algorithms, including artificial neural networks (ANN) and decision tree (DT) were tentatively applied for BD estimation of the studied soils, showing that the site-specific SR-based equation performed the best. Various soil properties were evaluated in the models, with soil organic matter and clay contents being the most significant contributors to the projection. Furthermore, the performance of the SR-based PTF was validated by comparison with 63 PTFs currently in use, which showed to perform poorly and vary widely in BD estimation for the hilly soils studied in this work. In conclusion, the SR equation and PTF developed in this work show excellent and promising suitability for stakeholders and professionals in the study area and for the global scientific community as a reliable BD estimator for hilly soils. Furthermore, the results of this work can be used for soil management, land use planning, and climate change mitigation in fragile ecosystems like the Himalayas.

Keywords Bulk density estimation · Hilly soils · Pedotransfer functions · Soil organic matter · Stepwise regression · Soil quality and vulnerability studies

1 Introduction

Soil bulk density (BD) exerts a relevant effect on several soil functions and processes, including water retention and transmission, compaction, structure, carbon sequestration, erosion, irrigation, and drainage (Popolizio et al. 2022). The development of plant roots and water movement is hindered by high BD values, mainly due to soil compaction. Various chemical properties, including cation exchange capacity, organic matter (OM) transformations, and nutrient mineralization and release, are influenced by soil BD

directly or indirectly (Abebe Ayalew 2020; Hijbeek et al. 2019; Mengesha & Tamiru 2018). Many biological properties, such as microbial population, enzyme activity, soil fauna, and root architecture, including their proliferation, are highly impacted by BD (Bansal et al. 2022).

Soil BD can be measured by using either direct or indirect methods. For large-scale applications, direct measurement methods based on core, clod, or excavation are labor-demanding, tedious, and time-consuming (Choudhury et al. 2023). On the other hand, indirect methods based on pedotransfer functions (PTFs) based on easily retrievable soil properties have become very common due to their affordability and rapidity (Nasta et al. 2020; Palladino et al. 2022). Sixty-three worldwide published PTFs that use regression or machine learning (ML) algorithms to estimate BD are available. However, existing PTFS have been developed for specific ecosystems and soil types, making them less reliable for the hilly North-Western Himalayas (NWH) area, where soil characteristics are markedly changeable owing to steep gradients, erosion vulnerability, and heterogeneous land-use patterns. (Nasta et al. 2020).

Methods based on PTFs to estimate BD have included more traditional ones, such as stepwise regression (SR), partial least-squares regression (PLSR), multiple linear regression (MLR), linear regression (LR), and have been strengthened over time by employing advanced ML algorithms, including artificial neural networks (ANN), random forests (RF), decision tree (DT) analysis, support vector machine (SVM), and others (Sharma et al. 2020). For example, Rodríguez-Lado and Martínez-Cortizas (2015) compared three methods, i.e., stepwise multiple linear regression (SMRL), RF and ANN, to map soil BD using a database of 115 topsoil measurements in a watershed of approximately 100 km^2, finding that the most performant method was ANN. Excellent results were achieved by Premrov et al. (2018) by employing appropriate power transformation of some soil chemical and physical properties. More recently, Choudhury et al. (2023) estimated soil BD in the eastern Himalayas by building land use-specific PTFs based on soil particle size and organic carbon (OC) data from 1206 sites spanning seven land uses. By employing five ML and multilinear regression methods, these authors found that ANN performed the best for grasslands and cultivated lands. At the same time, RF was most successful for forests and plantations, outperforming other algorithms like ridge regression. Although PTFs obtained by ML methods can achieve greater accuracy in BD prediction, local stakeholders, end-users and professionals would take advantage of the availability of simpler empirical regression equations to estimate soil BD.

For hilly ecosystems, direct measurements of BD are laborious, difficult for large areas with undulated terrain, and very expensive for sample collection and transportation. This is the primary reason to often leave over BD measurements in traditional soil surveys and fertility assessments. Most of these shortfalls can be overcome by achieving soil BD using a rapid and inexpensive PTF. The use of this approach for extensive inaccessible terrains, such as those in the western Himalayas, can help in soil and crop management at the regional scale, mainly related to soil compaction, proper hydrothermal regime, carbon sequestration, hydraulic properties, soil erosion, etc. Estimating soil BD is crucial in the NWH area due to the region's fragile ecosystems that are prone to soil erosion, landslides, and degradation (Das and Meher 2019; Kanungo and Sharma 2014). Accurate BD estimations are important for understanding soil compaction, water infiltration, and root penetration, all of which influence the agricultural productivity and slope stability in the terraced landscapes of NWH (Mourya et al. 2024; Nazir et al. 2022; Svoray 2022). Additionally, NWH plays a significant role in global carbon dynamics, making BD critical for quantifying soil organic carbon (SOC) stocks (Bashir et al. 2024a, b) and supporting climate change mitigation strategies, which are vital for managing water resources in NWH facing erratic rainfall and water scarcity. The region's complex topography, varied soil compositions, and fluctuating climate conditions complicate the use of direct measurement methods, making them laborious and time-consuming. Although PTFs obtained by ML methods can achieve greater accuracy in BD prediction, local stakeholders, end-users and professionals would take advantage of the availability of simpler empirical regression equations to estimate soil BD.

To address the lack of research on soil BD estimation in the NWH, this study aimed at developing a novel PTF suited for any kind of soil in hilly regions based on a critical evaluation of traditional regression techniques (PLSR, SR, LR, MLR) with respect to advanced machine-learning algorithms (ANN, DT). The main objective of this work was to undertake a rigorous evaluation using the coefficient of determination (R^2), the root mean square error (RMSE), and the mean absolute error (MAE) to confirm the performance of the developed PTF model in predicting BD of hilly soils by comparison with the PTFs available in the current literature.

The innovative aspect of this study consists in the development of a novel PTF tailored explicitly to the hilly NWH soils, which addresses a critical gap in the reliable BD estimation for this region. In particular, the SR-based model will be shown to be more robust, accurate and precise for hilly soils than the 63 PTFs available in the current literature. The innovative methodological advancement of the proposed PTF will enhance BD prediction for the NWH region and provide a scalable tool for global applications in soil quality assessments, resilience indicators, and digital soil mapping.

2 Materials and Methods

2.1 Study Area

The study area is located in the NWH region and covers an area of 6972 km^2 (Fig. 1). The region includes different landforms such as plains, valleys, hills and mountains, and various land uses, i.e., agriculture, horticulture, forest, and fallow (Fig. 1). The elevation varies from 1295 to 2500 m above the mean sea level (MSL). The climate is temperate, with temperatures ranging from −8.0 to 35 ^{0}C and dropping below zero in the winter, with moderate to heavy snow. The average annual rainfall ranges between 800 and 1100 mm, with March being the wettest month. The area features a

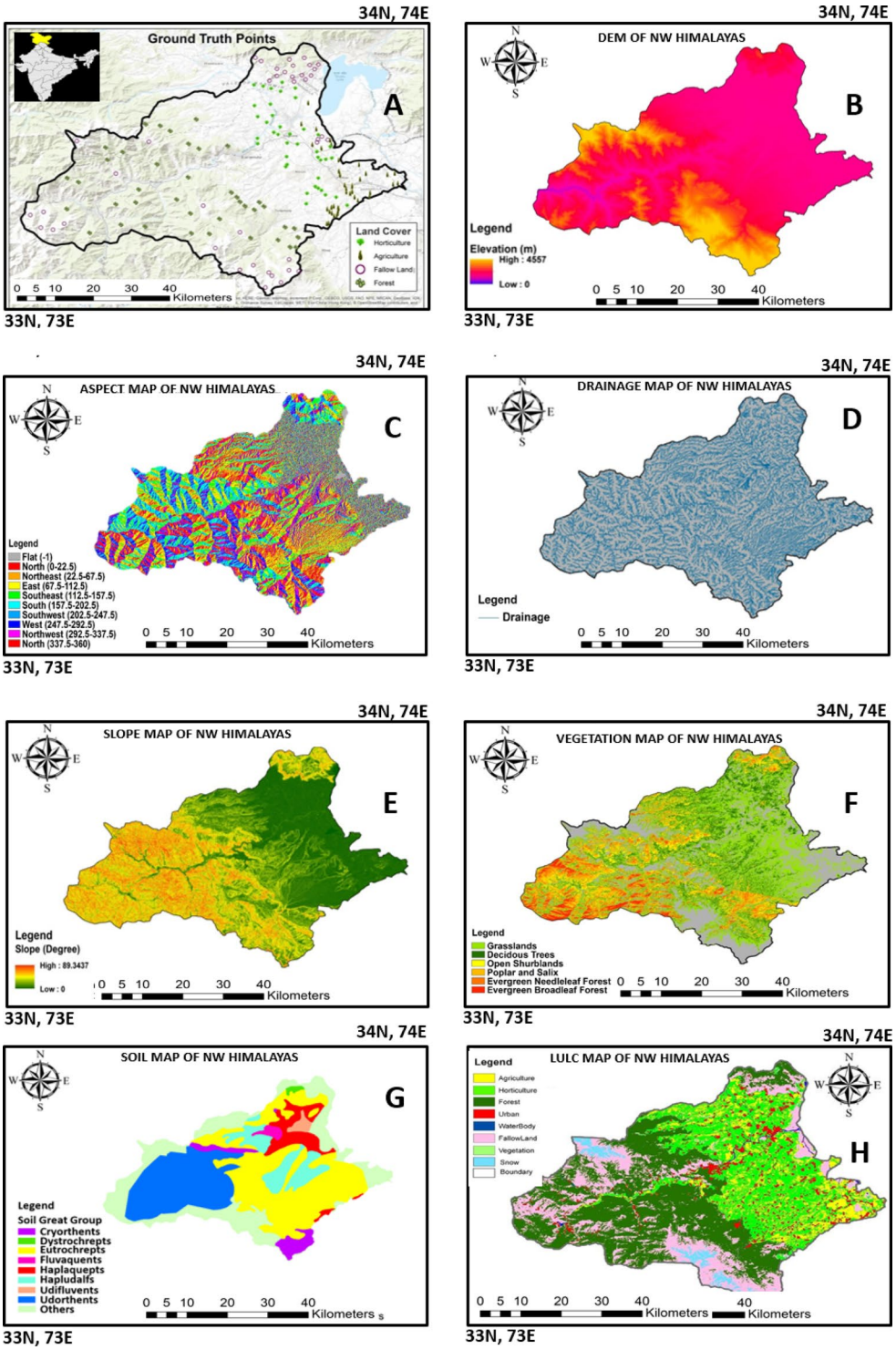

Fig. 1 The study area indicating the 300 sampling sites distinguished by land use type, Ground Truth Points (**A**), digital evaluation model (DEM) map (**B**), aspect map (**C**), drainage map (**D**), slope map (**E**); vegetation map (**F**); soil map (**G**); land use and land cover (LULC) map (**H**) (Bashir et al. 2024a, b)

mesic soil temperature and a udic soil moisture regime. The dominant soil orders are alfisols, inceptisols, and entisols. The dominant plant species include *Pinus Spp.*, *Fir Spp.*, *Cedrus spp.*, *Salix spp.*, *Populus spp.*, *and Ulmus spp.* (Bashir et al. 2022).

The dominant land use map refers to the year 2020 (Fig. 1H), and the corresponding land use classes, i.e., agriculture, horticulture, forest, and fallow (Fig. 1A), were identified according to CORINE land cover data (Bossard et al. 2000) by monitoring satellite and aerial photographs accessible through ArcMap and Google Earth-Pro.

2.2 Soil Sampling and Laboratory Analysis

A total of 75 disturbed and 75 undisturbed soil samples were collected randomly following a grid pattern of 500 × 500 m from the topsoil layer (0–30 cm depth) in each land use area, i.e., agriculture, horticulture, forest and fallow, for a total of 300 disturbed and 300 undisturbed samples. The disturbed soil samples were ground and sieved at 0.15 and 2.0 mm. The 0.15-mm sieved samples were used to measure soil OC by the dichromate method (Mebius 1960), whereas the 2.0-mm sieved samples were used to determine the textural distribution of soil particles, i.e., the percentages of sand (Sa), silt (Si), clay (Cl) and loam (Lo), according to the United States Department of Agriculture (USDA) method (Bernoux et al. 1998) (Fig. 2) and the soil classification protocol suggested by Gee and Or (2002). The undisturbed soil cores were collected using sharpened steel cylinders (diameter, 5 cm; height, 15 cm) and oven-dried at 105 °C for 24 h to measure their BD using Eq. 1.

$$BD = M_{0ds}/TV \quad (1)$$

where M_{0ds} is the Mass of oven Dry soil and TV is the total core volume.

2.3 Development of the Pedotransfer Function To Estimate Soil Bulk Density

Based on an extensive search, no study was found in the current literature on the estimation of soil BD using PTFs specifically for the NWH area. Thus, in this work, a specific PTF for soil BD of this area was developed by testing various methods, i.e., PLSR, SR, LR, MLR, ANN and DT (Sequeira et al. 2014; Xiangsheng et al. 2016). In this study, a 75:25 ratio was used as training and testing data sets. A K-fold cross-validation technique increased the model's accuracy and reliability. The Python 3.4 program was utilized to carry out extensive simulations with non-parametric methods. The scikit-learn open-source library for Python was used to train and test all the multiple linear predictive models considered in this study. In the past, no such study has been conducted in any hilly region worldwide, thus making any comparison impossible. Furthermore, as the dataset available for NWH is limited, the implementation of advanced machine learning algorithms like RF appears inadequate, as it needs a more extended dataset to avoid overfitting. Figure 3 represents the flowchart of the methodological process applied in this study.

The first step applied to estimate soil BD by various models was the selection of the most relevant predictor variables. As the soil texture and organic matter have the highest influence on soil BD, soil properties like sand, silt, clay and organic matter were identified as primary factors in BD estimation. The Variance Inflation Factor (VIF) method, which is widely used to detect the relationships among variables, ensuring the robustness and reliability of the selected predictors, was applied. As a high VIF score indicates a robust

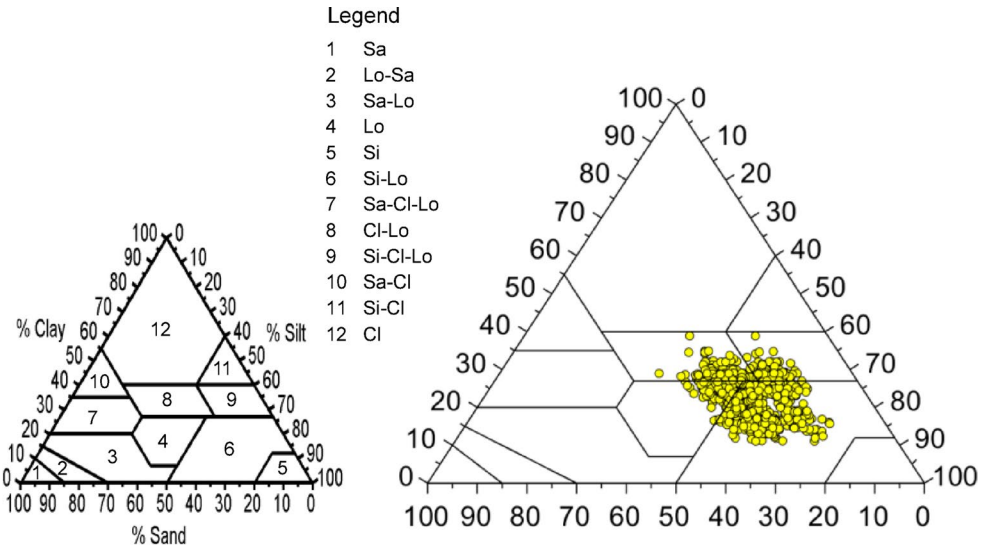

Fig. 2 Textural distribution of soil samples in the USDA texture triangle. Sa, Si, Cl and OM indicate sand, silt, clay and organic matter

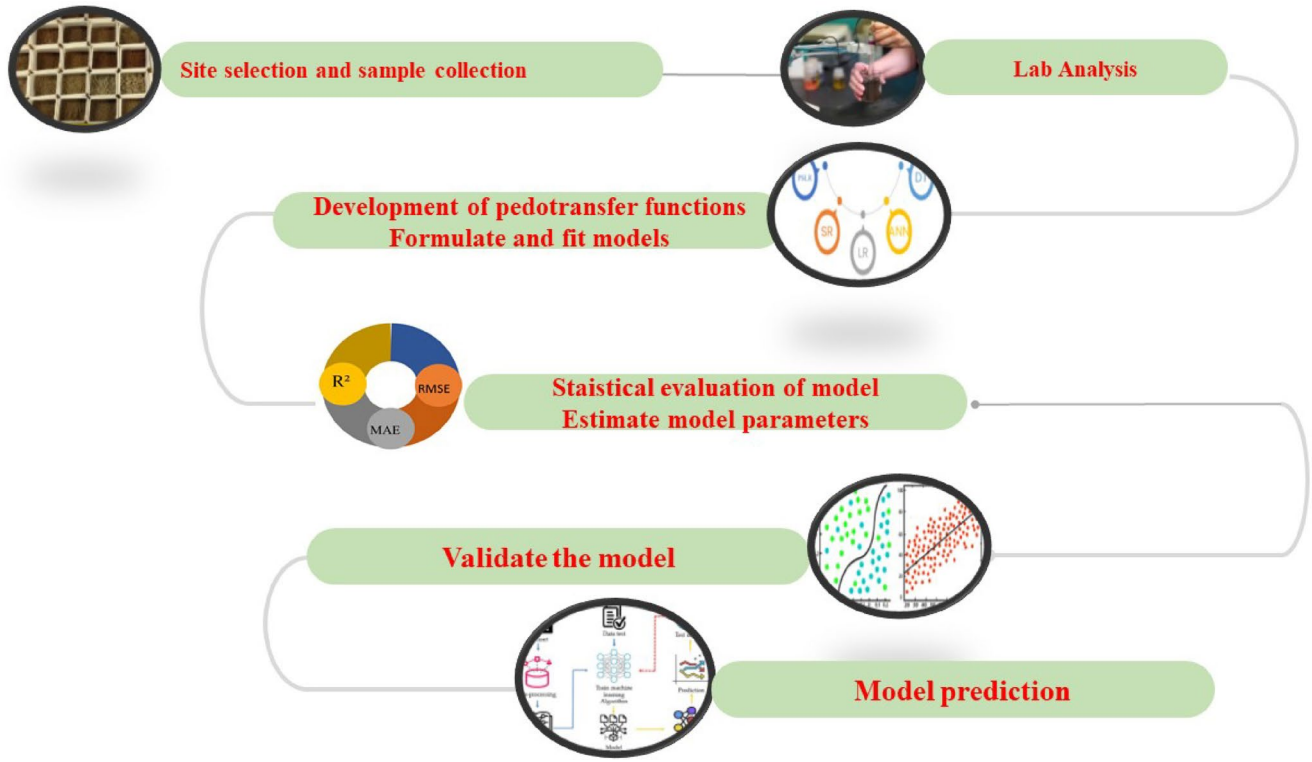

Fig. 3 Methodological flowchart of the study

relationship between the variables, those featuring high VIF scores were selected. Thus, the VIF process helped us enhance the model's predictive power and improve its overall performance.

2.3.1 Partial Least Square Regression (PLSR)

The PLSR model, which is an extension of the MLR model, was used to analyze the interaction between the four predictors (sand-Sa, silt-Si, clay-Cl, organic matter-OM) and the dependent variable BD, according to Eq. 2.

$$\mathrm{BD} = \beta_0 + \beta_1 \mathrm{Sa} + \beta_2 \mathrm{Si} + \beta_3 \mathrm{Cl} + \beta_4 \mathrm{OM} \quad (2)$$

where β_0 is the regression coefficient of the intercept, and β_i is the i-th regression coefficient of the four predictor variables.

The explained variance of BD was defined using PLSR by introducing new components that were linear combinations of the original predictor variables and finding the combinations of the predictors that showed a significant covariance with the dependent variable. The importance of a predictor was gauged in the PLSR model based on its variable importance in the projection (VIP). The most relevant predictors for explaining the dependent variable were assumed to be those with high VIP values. With this regard, Wold (1978) proposed that predictors with a VIP > 0.8 are the most influential for interpreting the dependent variable, while those with a VIP < 0.5 are considered of minor relevance.

2.3.2 Stepwise Regression (SR)

In the SR method, a regression model was constructed step-by-step, and potential explanatory variables were added or removed by evaluating their statistical significance at each step. The variable that generated the most significant rise in R^2 was the first one included in the model, i.e., when the partial Fisher (pF) test showed a substantial increase in the explained variance, the variable was kept in the forward step, whereas leaving this variable out in the backward step reduced the explained variance the least. If the explanatory variable decrease was not statistically significant at a sure PF and exceeded the threshold incorporated, it was excluded by the model. The procedure was completed when no more response variables were added or removed (Noryani et al. 2019). Regression residuals were generated using the Kolmogorov-Smirnov normality and Breush-Pagan tests for variance homogeneity (Breusch and Pagan 1979).

Mathematical transformations were applied to expand the number of both independent and primitive variables. These included square and cubic power, square and cubic root, logarithmic multiplications (Sa x Si, Sa x Cl, Sa x OM,

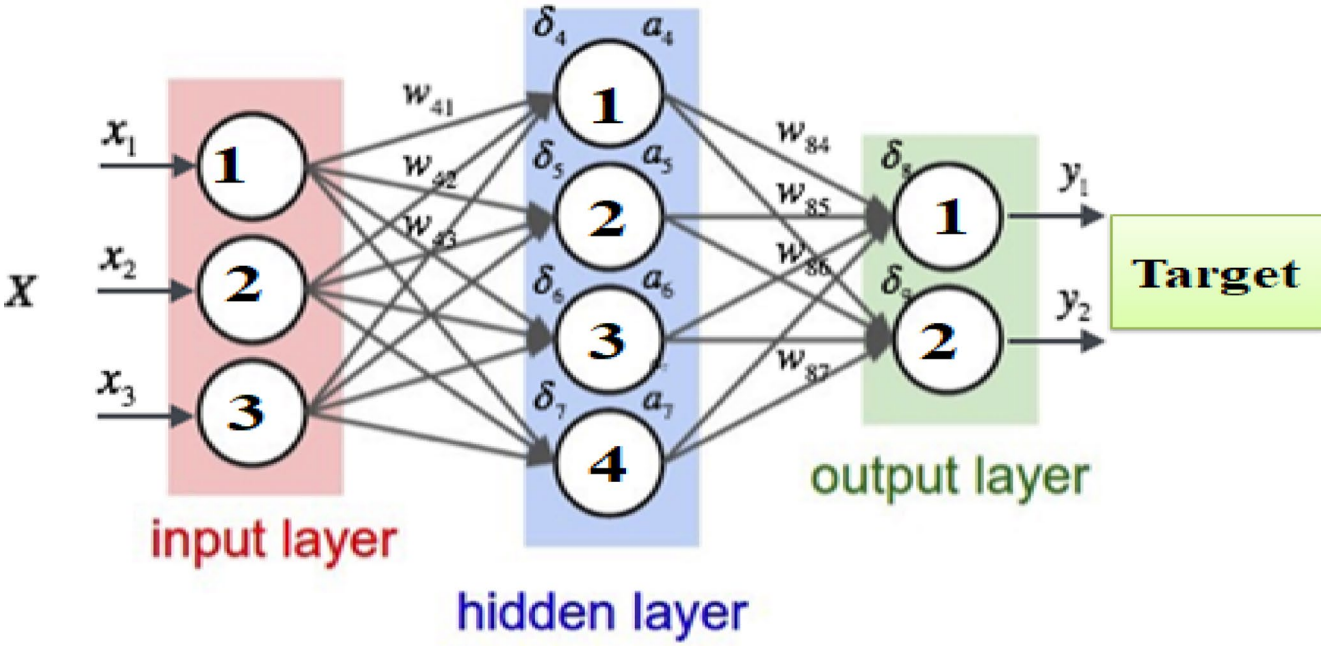

Fig. 4 ANN model hierarchy

Si x Cl, Si x OM, and Cl x OM), and ratios of variables (Sa/OM, Si/OM, and Cl/OM). The SR results showed that the most predictive variables in this case study were $\log_{10}$(OM), Cl x OM, and Cl/OM. Thus, the predictive equation resulted in the following:

$$\mathrm{BD} = \mathrm{a} + \mathrm{b} \times \log_{10}(\mathrm{OM}) + \mathrm{c} \times \mathrm{CI} \times \mathrm{OM} + \mathrm{d} \times \mathrm{CI/OM} \quad (3)$$

where a, b, c and d are the regression coefficients to be optimized.

The SPSS v.23 and Matlab v.2019 methods were used for all mathematical and statistical editing of PTFs.

2.3.3 Linear Regression (LR) and Multiple Linear Regressions (MLR)

A prediction based on the LR approach can be achieved by creating a linear equation with a specific set of input values (x) to predict the output values (y). The MLR approach consists of a systematic method that starts with a no response variable (a constant-only model), and the first response variable in the model is considered the one that produces the highest increase in R^2. If the pF test shows a significant increase in explaining variance, the model includes the variable (forward step). The process is repeated for evaluating another independent variable, and so on. At each step, the variable that reduces the explained variance the least is omitted. The model does not include any explanatory variable whose decrease is not statistically significant at a particular pF and exceeds the incorporated threshold. The procedure is completed when no more response variable is added or deleted, as mentioned by (Noryani et al. 2019). The Kolmogorov-Smirnov normality and the Breush-Pagan tests for variance homogeneity were used to evaluate regression residuals (Breusch and Pagan 1979).

2.3.4 Artificial Neural Network (ANN)

The ANN method involves a computing system that can replicate the information processing mechanisms of the human brain, i.e., the identification of non-linear patterns that cannot be detected using traditional regression-based methods. A PTF is typically constructed using a multi-layer perceptron (MLP) architecture that features an input, hidden, and output layer. The log and min-max transformation methods were used to normalize data for all ML models, including ANN. In this work, four input predictors and one output variable, which is BD, were used in the MLP. The best MLP performance was achieved by the Python 3.4 software using a hidden layer of three neurons and the hyperbolic tangent activation function, which matched the software's default settings. The output layer was used because of a regression problem caused by the identity function. The model training took only a few sec. The iterative tuning of the hyperparameters was done by testing different configurations of the ANN. Both a single hidden layer and two to ten neurons and two hidden layers and a variable number of neurons in the first layer (two to five) and in the second layer (two or three) were tested (Fig. 4). The use of one hidden layer resulted more performant than two hidden layers.

Table 1 Accuracy criteria (MAE, RMSE, and R^2) used to evaluate the PTF developed in this work and those available in the literature

Accuracy criteria	Equations
MAE	$MAE = \frac{1}{n}\sum_{i=1}^{n}\lvert O_i - P_i\rvert$
RMSE	$RMSE = \sqrt{\frac{1}{n}\sum_{i=1}^{n}(O_i - P_i)^2}$
R^2	$R^2 = 1 - \left(1 - \frac{\sum_{i=1}^{n}(O_i - P_i)^2}{\sum_{i=1}^{n}\left(O_i - \bar{O}\right)^2}\right)$

The symbols O, $\bar{O}$, and P refers to the measured BD, the average measured BD, and the predicted BD, respectively; *i* refers to each soil sample, and *n* represents the total number of soil samples

2.3.5 Decision Tree (DT)

The ensemble DT method is a type of supervised learning that does not involve parameters and can be applied to classification and regression. A DT structure resembles a flowchart, with each node in the tree being a test for a feature and each leaf node being a class label created by a combination of features in each branch. An algorithm is employed to construct a DT model by exploring ways to divide data based on different conditions. Supervised learning is one of the most common and valuable ways to achieve it. This work used four nodes with eight branches in the class label. The bootstrap method determines the number of trees' values, which vary with every iteration. As such, reasonable predictions did yield within 150 to 200 trees value.

2.4 Statistical Evaluation

Three accuracy indicators, i.e.: (i) the coefficient of determination (R^2), (ii) the root mean square error (RMSE), and (iii) the mean absolute error (MAE) (Table 1) (Han et al. 2012; Nanko et al. 2014), were used to evaluate the performance of BD predictive models. These metrics provide a robust assessment of the strength (R^2) and predictive accuracy (RMSE, MAE), making them highly effective. However, additional metrics like bias and residual analysis would have provided further insights into this study.

The R^2 coefficient was used to evaluate the scatter plot of predicted values against observed values. The bias magnitude and its percentage were calculated from $+\infty$ to $-\infty$. Although the optimal bias percentage is 0, a value of less than 10% is generally considered satisfactory. The optimal value of the calculated RMSE and % RMSE would be, respectively, 0 and from 0 to $+\infty$. However, a % RMSE lower than 10% is considered satisfactory.

The Pearson correlation coefficients were also computed from +1 to −1, with an optimal value of 1. Finally, the regression slope between the experimental and estimated data was calculated in the range +/- ∞, with an optimal value of 1. The optimal prediction is indicated by a value of 0 for MAE and RMSE and 1 for R^2. However, De Vos et al. (2005a, b) suggested that the model performance is acceptable if RMSE ranges between 0.12 and 0.25.

2.5 Model Performance Evaluation

To assess the performance of the newly developed PTF, each of the 63 PTF equations available in the literature (Table 2) (Nasta et al. 2020) was applied to the 300 soil samples examined in this work, and the data achieved were subjected to the three accuracy criteria mentioned above (Table 2). For example, Abdelbaki (2016) applied 48 available PTFs to the largest soil database in the USA using 45,195 samples. Xiangsheng et al. (2016) evaluated the predictive performance of 14 PTFs on 495 alpine samples collected from 100 different soil profiles in the Three-River Headwaters area, China. Choudhury et al. (2023) evaluated the performance of 13 published PTFs and seven developed PTFs on 1206 acidic topsoils from Eastern Himalaya, India. Boschi et al. (2018) applied and evaluated 25 PTFs to a data set comprising 884 soil samples from Brazil. Nasta et al. (2020) applied 63 PTFs to 3316 Italian soils, and Sevastas et al. (2018) 56 PTFs to 30 Greek soils. In these studies, the regression analysis was based only on the OC content and soil texture, as these parameters were found to have the most significant impact on soil BD and be easily accessible (Abdelbaki 2016; Hollis et al. 2012; Manrique and Jones 1991).

A novel PTF needed to be developed as the described PTFs were designed for different locations and exhibited inadequate performance when applied to the distinct soil properties of the NWH region. In particular, the variability of organic matter, clay and sand composition in the hilly landscapes of this area necessitates the development and use of a region-specific PTF to enhance the accuracy of soil bulk density (BD) estimations. The PTFs were edited using SPSS v.23 and Matlab v.2015 methods.

3 Results and Discussion

3.1 BD Measurements

The histograms of the measured soil BD values did not exhibit a normal frequency distribution (Fig. 5), which was confirmed by the Lilliefors test that disproved the null hypothesis of normality at a 5% significance level. The experimental data's minimum, maximum, mean, median and standard deviation were 1.09, 1.57, 1.31, 1.33, and 0.094 g cm^{-3}.

Table 2 Equations of the 63 published PTFs (in alphabetical order of authors) applied to the 300 soils examined in this work

Authors	Equations	No. of samples	Location	Land use
Abdelbaki (2016)	$BD = 1.449 \times e^{(-0.03 \times OC)}$	45,000	USA	NA
Adams (1973)	$BD = \frac{100}{\frac{OM}{0.244} + \frac{100-OM}{1.27}}$	77	UK	Forest
Akpa et al. (2016)	$BD = 1.177 + 0.00263 \times Sa - 0.0439 \times \log(Si) + 0.00208 \times Si$	2124	Nigeria	Multiple
Alexander (1980)	$BD = 1.66 - 0.308 \times (OC)^{0.5}$	721	USA	Upland
Alexander (1980)	$BD = 1.72 - 0.294 \times (OC)^{0.5}$	721	USA	Alluvial
Al-Qinna and Jaber (2013)	$BD = 1.228 - 0.155 \times \log_{10}(OC) + 0.008 \times Sa$	332	Jordan	Multiple
Benites et al. (2007)	$BD = 1.5688 - 0.0005 \times (Cl \times 10) - 0.009 \times (OC \times 10)$	1396	Brazil	Multiple
Bernoux et al. (1998)	$BD = 1.398 - 0.0047 \times Cl - 0.042 \times OC$	323	Brazil	Multiple
Beutler et al. (2017)	$BD = [1.6179 - 0.018 \times (Cl+1)^{0.46} - 0.0398 \times OC^{0.55}]^{1.33}$	280	Brazil	Multiple
Botula et al. (2015)	$BD = 1.64581 - 0.00362 \times Cl - 0.0016 \times Sa - 0.0158 \times OC$	196	Africa	Multiple
Calhoun et al. (2001)	$BD = 1.673 - 0.071 \times OC - 0.0017 \times Si - 0.003 \times Cl$	937	USA	Multiple
Cienciala et al. (2006)	$BD = \frac{100}{\frac{OM}{0.244} + \frac{100-OM}{1.41}}$	360	Czech Republic	Forest
Curtis and Post (1964)	$BD = 10^{[2.09963 - 0.00064 \times \log10(OM) - 0.22302 \times \log10(OM)2]}$	NA	USA	Forest
De Vos et al. (2005a, b)	$BD = 1.775 - 0.173 xOM^{0.5}$	1614	Belgium	Forest
Dexter (2004)	$BD = \frac{1}{(0.59 + 0.00163Cl + 0.0253OM)}$	119	Germany	NA
Drew (1973)	$BD = \frac{1}{(0.6268 + 0.0361OM)}$	156	USA	Forest
Eschner et al. (1957)	$BD = 1.8014 - 0.8491 \times \log_{10}(OM+2) + 0.0026 \times Cl$	134	USA	Multiple
Federer (1983)	$BD = \exp[-2.314 - 1.0788 \times \ln(OM/100) - 0.1132 \times \ln(OM/100)^2]$	NA	USA	Forest
Federer et al. (1993)	$BD = \frac{0.111 \times 1.45}{1.45 \times \frac{OM}{100} + 0.111 \times (1 - \frac{OM}{100})}$	148	USA	Forest
Grigal et al. (1989)	$BD = 0.075 + 1.301 \times e^{(-0.06 \times OM)}$	171	USA	Forest
Hallet et al. (1998)	$BD = 0.87 + 0.071 \times \ln(Cl) + 0.093 \times \ln(Sa) - 0.254 \times \log(OC)$	1568	UK	Multiple
Hallet et al. (1998)	$BD = 1.46 + 0.0254 \times \ln(Cl) + 0.0279 \times \ln(Sa) - 0.261 \times \ln(OC)$		UK	Multiple
Han et al. (2012)	$BD = e^{(0.5379 - 0.0653 \times (OM)\text{^}0.5)}$	502	China	Forest
Harrison and Bocock (1981)	$BD = 1.558 - 0.728 \times \log_{10}(OM)$	539	UK, Sweden	Multiple
Heuscher et al. (2005)	$BD = 1.711 - 0.0487 \times OC^2 + 0.0059 \times OC^3 + 0.002 \times Cl$	619	USA	Vertisols
Heuscher et al. (2005)	$BD = 1.674 - 0.31 \times OC^{0.5} + 0.015 \times Cl - 2.41e\text{-}4 \times Si^2$	13,600	USA	Alfisols
Hollis et al. (2012)	$BD = 1.780 - 0.379 \times OC^{0.5} + 0.00123 \times depth$	13,600	USA	Alfisols
Hollis et al. (2012)	$BD = 0.80806 + 0.823844 \times e^{(-0.27993 \times OC)} + 0.0014065 \times Sa - 0.0010299 \times Cl$	67	Europe	Multiple
Hollis et al. (2012)	$BD = 0.69794 + 0.750636 \times e^{(-0.230355 \times OC)} + 0.0008687 \times Sa - 0.0005164 \times Cl$	1545	Europe	Multiple
Hollis et al. (2012)	$BD = 1.4903 - 0.33293 \times \ln(OC)$	67	Europe	Multiple
Honeysett and Ratkowsky (1989)	$BD = \frac{1}{0.564 + 0.556 \times OM}$	136	Tasmania	Multiple
Hong et al. (2013)	$BD = 100/\{OM/0.224 + [(100\text{-}OM)/1.017] + 0.0032 \times Sa + 0.054 \times \log_{10}(depth)\}$	642	Global	NA
Hossain et al. (2015)	$BD = 0.701 + 0.952e^{(-0.29 \times OC)}$	702	Canada	NA
Huntington et al. (1989)	$BD = e^{\{-2.39 - 1.316 \times \ln(\frac{OM}{100}) - 0.167 \times [\ln(\frac{OM}{100})]\text{^}2\}}$	60	USA	Forest
Jeffrey (1970)	$BD = 1.482 - 0.6786 \times \log_{10}(OM)$	80	Australia, England	Multiple
Kaur et al. (2002)	$BD = e^{(0.313 - 0.191 \times OC + 0.02102 \times Cl - 0.000476 \times Cl\text{^}2 - 0.00432 \times Si)}$	224	India	Multiple
Keller and Håkansson (2010)	$BD = 1.308 + 0.0119 \times Cl + 0.0103 \times Sa\text{-}0.00018 \times Cl^2 - 0.00008 \times Sa^2 - 0.00062 \times Si \times OM - 0.00059 \times Sa \times OM$	175	Sweden	Multiple
Kobal et al. (2011)	$BD = 1.4842 - 0.1424 \times OC$	109	Slovenia	Forest
Leonaviciute (2000)	$BD = 1.70398 - 0.00313 \times Si + 0.00261 \times Cl\ \text{-}0.11245 \times OC$	140	Lithuania	NA
Manrique and Jones (1991)	$BD = 1.51 - 0.113 \times OC$	19,651	USA	Multiple
Men et al. (2008)	$BD = 1.386 - 0.078 \times OC + 0.001 \times Si + 0.001 \times Cl$	NA	NA	NA
Valzano et al. (2005)	$BD = 1.608 - 0.0872 \times OC$	NA	Australia	NA
Minasny and Hartemink (2011)	$BD = 100/\{OM/0.224 + (100\text{-}OM)/[0.935 + 0.049 \times \log_{10}(depth) + 0.0055 \times Sa + 0.000065 \times (Sa\text{-}38.96)^2]\}$	670	Global tropics	NA
Nanko et al. (2014)	$BD = \frac{100}{\frac{OM}{0.244} + \frac{(100-OM)}{1.269}}$	3513	Japan	Forest
Palladino et al. (2022)	$BD = 1.131 + 0.00299 \times Sa + 0.0051158 \times Cl\text{-}0.0388105 \times OC$	3316	Italy	Multiple

Table 2 (continued)

Authors	Equations	No. of samples	Location	Land use
Perie and Ouimet (2008)	$BD = \frac{(0.1111.767)}{1.767\frac{OM}{100}+[(1-\frac{OM}{100})\,0.111]}$	157	Canada	Forest
Prévost (2004)	$BD = e^{[-1.81-0.892\times\ln\left(\frac{OM}{100}\right)-0.092\times\ln\left(\frac{OM}{100}\right)^2]}$	NA	Canada	Forest
Rawls et al. (2004)	$x = -1.2141+4.23123\times Sa/100$; $y = -1.70126+7.55319\times Cl/100$; $z = -1.55601+0.507094\times OM$; $w = -0.0771892+0.256629\times x+0.256704\times x^2-0.140911\times x^3-0.0237361\times y-0.098737\times x^2\times y-0.140381\times y^2+0.0140902\times x\times y^2+0.0287001\times y^3$; $BD = 1.36411+0.185628\times(0.0845397+0.701658\times w-0.614038\times w^2-1.18871\times w^3+0.0991862\times y-0.301816\times w\times y-0.153337\times w^2\times y-0.072242\times y^2+0.392736\times w\times y^2+0.0886315\times y^3-0.601301\times z+0.651673\times w\times z-1.37484\times w^2\times z+0.298823\times y\times z-0.192686\times w\times z\times y+0.0815752\times y^2\times z-0.0450214\times z^2-0.179529\times w\times z^2-0.0797412\times y\times z^2+0.00942183\times z^3)$	2100	USA	Multiple
Reidy et al. (2016)	$BD = 1.705925–0.342497\times OC^{0.5}$	2950	Ireland	NA
Ruehlmann and Körschens (2009)	$BD = (2.684-140.943\times 0.008)\times e^{(-0.008\times OC\times 10)}$	2100	Global data	Arable lands
Saini (1966)	$BD = 1.53–0.05\times OM$	40	USA	NA
Sevastas et al. (2018)	$BD = 2.268–0.179\times\ln(Sa)-0.345\times\ln(OC)$	32	Greece	Multiple
Sevastas et al. (2018)	$BD = 2.039–0.563\times OC+0.103\times OC^2$	32	Greece	Multiple
Song et al. (2005)	$BD = 1.3565\times e^{(-0.0046\times OC\times 10)}$	3645	China	Uncultivated
Song et al. (2005)	$BD = 1.3770\times e^{(-0.0048\times OC\times 10)}$	3645	China	Uncultivated
Tamminen & Starr (1994)	$BD = 1.565–0.2298\times OM^{0.5}$	158	Finland	Forest
Tomasella and Hodnett (1998)	$BD = 1.578–0.054\times OC-0.006\times Si-0.004\times Cl$	396	Brazil	NA
Tranter et al. (2007)	$BD = 1.35+0.0045\times Sa+(44.7-Sa)^2\times 6e^{-5}+\ln(depth)$	926	Australia	Multiple
Tremblay et al. (2002)	$BD = \frac{(0.121.4)}{\frac{OM}{100}+\left[\left(1-\frac{OM}{100}\right)\times 0.12\right]}$	281	Canada	Forest
Williams (1971)	$BD = 1.37–0.076\times OC$	37	UK	Grasslands
Wu et al. (2003)	$BD = 1.2901–0.1229\ln(OC)$	784	China	Multiple
Yang et al. (2007)	$BD = 0.29+1.2033e^{(-0.075\times OC)}$	4860	China	Multiple
Zinke et al. (1986)	$BD = 1.446–0.000645\times depth-0.344\log_{10}(OC)$	788	Mediterranean basin	Multiple

Soil bulk density, organic carbon, sand, silt And clay are denoted as BD, OC, Sa, Si, And Cl, respectively. OM denotes organic matter (OM = OCx1.724). And depth is the mean depth of the soil sample (15 cm)

The descriptive statistics of BD, OC, Sa, Si and Cl of soils under the various land uses, i.e., agriculture, horticulture, forest and fallow, are listed in Table 3. The soil parameters with the highest variability were BD and Cl, which exhibit CV values from 0.05 to 0.13 and 0.08 to 0.23, respectively. Soils under forest showed the lowest average BD values and OC content, whereas agricultural and fallow soils had the highest Cl content. These findings are in accordance with previous studies (Sharma et al., 2024; Hasan et al., 2025) in which forest soils featured lower BD due to minimal soil disturbance and higher OC accumulation.

The correlation coefficients between the measured soil variables are shown in Table 4. Noteworthy, a strong negative correlation was evident between BD and OC content confirming the inverse relationship found by Kahsay et al. (2025). The Sa content showed weak correlation with BD suggesting that the texture had dominate relevance lower than OC, which contradicts with the findings of Talat et al. (2025) for semiarid and arid tropical soils where the Sa fraction strongly influences BD.

The results obtained revealed a significant variation of OC, soil texture and BD across various land uses in the NWH soils. In particular, BD ranged from 1.1 to 1.6 g cm^{-3}, with soils under agricultural land use exhibiting the highest BD due to frequent tillage and reduced OC and the forest soils showing the lowest BD and higher OC content. Similar trends were observed by Gubila et al. (2024) and Chen et al. (2025) who found soil BD varying with various land use.

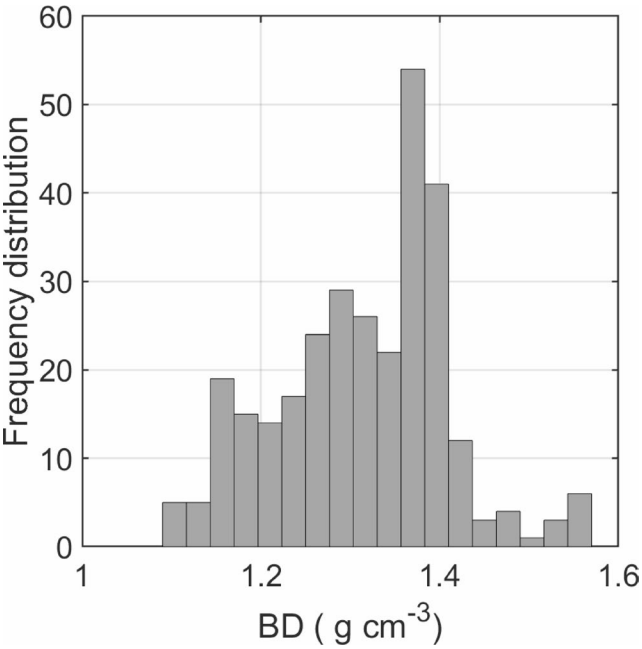

Fig. 5 The frequency distribution of the bulk density (BD) measured for the examined soil samples

The soil texture ranged from sandy loam to loam with the highest Cl percent in fallow and agricultural soils and the highest Sa content in forest soils. Furthermore, theCl content was positively correlated with the OC content, suggesting that the finer soil particles stabilize soil OC. These results agree with those of Barnard et al. (2025) and Al Shoumik et al. (2025), suggesting that soil Cl protects soil OC through aggregate formation.

Table 4 Correlation coefficients

	BD	Sa	Si	Cl	OC
BD	1				
Sa	− 0.126*	1			
Si	0.046	− 0.672**	1		
Cl	0.077	− 0.204**	− 0.588**	1	
OC	− 0.841**	0.087	− 0.108*	0.047	1

* Correlation significant at the 0.05 level; ** Correlation significant at the 0.01 level

The relationships between BD, soil texture and OC highlight the importance of these parameters in enhancing soil structure, water infiltration, and root growth. The conservation of soil OC under different land uses can mitigate soil compaction, improve resilience and contribute to carbon sequestration, so contributing to mitigate climate changes in mountainous regions.

3.2 Model Performance and Transferability

3.2.1 The PLSR Model

The results of PLSR analysis showed that Sa, Si, Cl, and OC were the four predictors that explained 72.2% of BD variation. The most significant predictor was OC, which had a VIP of 1.96, whereas the three texture classes, i.e., Sa, Si, and Cl, showed VIP values lower than 0.5. The OC explained 70.7% of BD variability if Sa, Si, and Cl were removed from the PLSR. Figure 6 shows the scatter plot between measured and estimated BD values, which featured a MAE of 0.0379 g cm^{-3}, a RMSE of 0.0487 g cm^{-3}, and a

Table 3 Descriptive statistics of soil parameters used to develop the PTFs (n: number of soil samples examined)

Land use	Soil parameters	*N*	Min	Max	Mean	SD	CV
Agriculture	BD (gcm^{-3})	75	1.39	1.57	1.46	0.21	0.09
	OC (%)	75	1.34	1.56	1.68	0.39	0.21
	Sa (%)	75	11.12	14.09	8.56	2.88	0.17
	Si (%)	75	38.72	56.92	51.23	7.97	0.32
	Cl (%)	75	23.13	34.77	26.03	4.69	0.23
Horticulture	BD (gcm^{-3})	75	1.33	1.49	1.37	0.18	0.12
	OC (%)	75	1.48	2.27	1.88	0.32	0.17
	Sa (%)	75	12.09	19.09	14.16	3.45	0.5
	Si (%)	75	56.00	67.98	61.24	5.89	0.39
	Cl (%)	75	15.78	31.44	26.03	5.07	0.21
Forest	BD (gcm^{-3})	75	1.09	1.34	1.22	0.12	0.05
	OC (%)	75	1.68	2.64	2.14	0.27	0.11
	Sa (%)	75	17.16	34.57	25.87	3.71	0.41
	Si (%)	75	51.04	72.54	59.10	12.12	0.47
	Cl (%)	75	18.09	30.63	24.29	5.97	0.18
Fallow	BD (gcm^{-3})	75	1.23	1.40	1.34	0.11	0.13
	OC (%)	75	1.14	2.21	1.68	0.31	0.06
	Sa (%)	75	16.88	24.25	21.07	3.14	0.43
	Si (%)	75	62.43	72.06	68.11	5.98	0.22
	Cl (%)	75	24.14	32.09	29.88	5.67	0.08

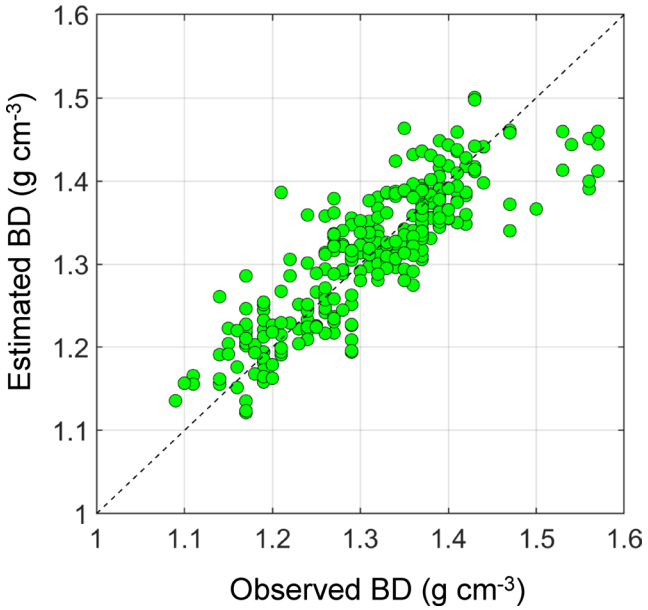

Fig. 6 Measured vs. SR-estimated soil bulk density (BD) values of the studied soils

R^2 of 0.73. Thus, the SR algorithm developed for the PTF of the samples studied in this work was the following:

$BD = 1.757 - 1.782 \times \log_{10}(OC) + 0.003401 \times Cl \times OC - 0.00797 \times Cl/OC$ (Eq. 4).

The model performance achieved for the soil samples studied was then validated using MAE, RMSE and R^2 values by applying Eq. 3 to the 63 published PTFs (Table 2), which were ranked hierarchically according to their RMSE values (Fig. 7). Noteworthy, 24 out of 63 PTFs achieved an excellent performance (RMSE < 0.12 g cm^{-3}), 27 PTFs were fair with an RMSE within the required range of 0. 12–0. 25 g cm^{-3} (De Vos et al. 2005a; Vos et al. 2005b), whereas the remaining 12 PTFs yielded poor performance (RMSE > 0.25 g cm^{-3}). The PTF used by Jeffrey (1970) performed the best and achieved the most accurate BD predictions (MAE = 0.05119 g cm^{-3}, RMSE = 0.064904 g cm^{-3}, $R^2 = 0.71$). This PTF was closely followed by those of Prévost (2004), Harrison and Bocock (1981), and Kobal et al. (2011), whereas the performances of the PTFs developed by Beutler et al. (2017), Heuscher et al. (2005), and Adams (1973) were the least performing. However, these results were not unexpected as the datasets used by these authors were acquired on arid soils that were low in OC, whereas the soils used in this study were rich in OC, which was shown to have a marked influence on BD values.

3.2.2 Non-parametric Models

Non-parametric models were tested using the Kalmogorov-Smirvon, and Breush-Pagan approaches to assess their homogeneity of variance and normality. The highest R^2 value (0.8972) was shown by the LR model, followed by MLR (0.8241) and DT (0.7621), and the lowest (0.6952) was recorded for the ANN model (Table 5). The RMSE values increased in the order: 0.1225 for the MLR model, 0.129 for LR, 0.2255 for the DT and 0.239 for ANN with bias values near zero (Table 5). Noteworthy, Cl and OC were the parameters that had the highest impact on soil BD evaluation.

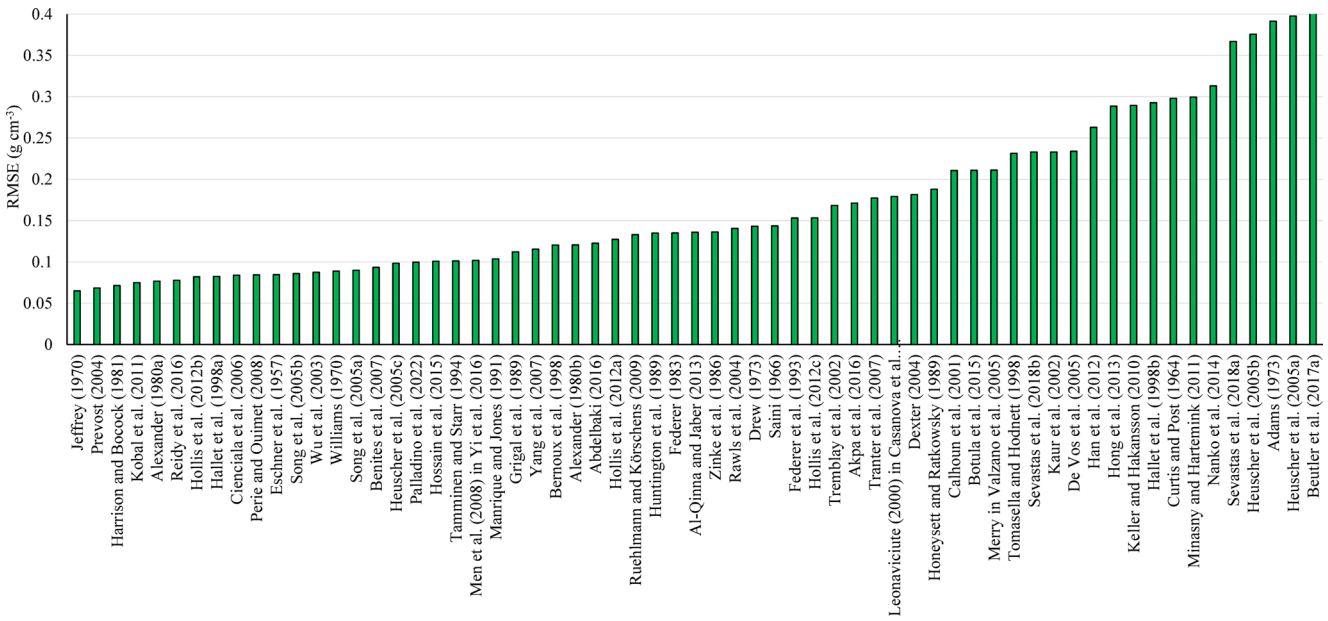

Fig. 7 Performance for BD estimation of the 63 published PTFs ranked from left to right according to their decreasing RMSE value

Table 5 Statistical parameters achieved by the various machine-learning models utilized to analyze the 300 samples in this work

Statistics	LR	MLR	DT	ANN
R^2	0.8972	0.8241	0.7621	0.6952
RMSE	0.129	0.1225	0.2255	0.239
% RMSE	8.45	7.34	6.32	5.89
Bias	0.0006	0.0011	0.0006	0.0009
% Bias	0.0023	0.0042	0.0013	0,0041
Estimated Max values	1.57	1.64	1.47	1.65
Estimated *Min values*	1.15	1.03	1.21	0.09

3.2.3 Comparison of Modelling Methods

The above-described results indicated that the model performance in predicting BD increased significantly using the *regression* algorithms. In particular, MLR performed better than ANN and DT models, with LR being the machine algorithm most frequently used (Schillaci et al. 2021). ANN has not always performed better (Tranter et al. 2007; Minasny and Hartemink 2011) and its evaluations were often ambiguous and subjective. However, unlike LR, ANN was able to provide specific models and regression coefficients for analyzing predictors. Probably, the underperformance of the ANN in predicting BD is due to the limited data sets available, as advanced ML require large datasets for a good generalization. Feature selection, scaling and overfitting can be other reasons that may impact the performance of ANN, as it is sensitive to input variables and to the high variability of the relatively small datasets. Additionally, ANN models require extensive hyperparameter tuning, thus they behave less effectively than MLR and LR that feature a linear nature of BD relationships (Hussen et al. 2024). The only studies that compared these models were those of Al-Qinna and Jaber (2013) and Sevastas et al. (2018), whose findings indicated that ANN was inferior to MLR. These results could be due to: (i) the significant difference in soil properties such as BD, OC and texture datasets among the various land uses; and (ii) the need to standardize data before ML calibration. The regression coefficients would be affected if the units and the order of magnitudes of OC content and textural data differ.

3.2.4 Development of a New PTF for Soils of Hilly Regions

The SR-based PTF developed and proposed in this study to evaluate soil BD shows potential applicability to other worldwide mountainous areas with similar soil composition and structural characteristics. The versatility of the model built using NWH soil data is based on its dependence on soil properties, such as OC, Cl and Sa contents, typical of hilly locations worldwide. The results of this research suggest that, with slight modifications, the developed PTF may provide a convincing basis for BD calculation in diverse hilly landscapes, facilitating the development of BD databases crucial for soil quality assessment, land-use planning, and worldwide carbon sequestration initiatives. Furthermore, the results of this study facilitate future research on soil vulnerability, resilience, and digital mapping by offering a framework reproducible for biomass density assessment in various hilly landscapes.

Furthermore, the value of the PTF developed in this study is confirmed by the thorough comparison with 63 previous PTFs, which inadequately estimate the BD of hilly soils of the region. The enhanced accuracy ($R^2 = 0.73$, MAE = 0.0379 g cm^{-3}, RMSE = 0.0487 g cm^{-3}) of the newly developed PTF constructed from site-specific data derived from 300 soil samples confirms the performance of the SR and PLSR methods applied to locally relevant soil properties such as OC, and addresses the shortcomings of current PTFs by positioning it as an innovative, promising solution for this particular environment.

3.3 Importance of Soil Predictors in Explaining BD Variability

The OCor OM content appeared to be the most significant factor in PLSR analysis, as also suggested by past studies (Palladino et al. 2022; Ramcharan 2017; Shiri et al. 2017). A negative correlation coefficient was reported between OM and BD, i.e., an increase in OM was related to a decrease in BD, with a simultaneous increase in soil porosity (Al-Qinna and Jaber 2013; De Vos et al. 2005a; Vos et al. 2005b; Tranter et al. 2007). Several studies have confirmed that PTFs based on soil OM content as the unique predictor were appropriate and could be used as a satisfactory alternative method for estimating soil BD (Chen et al. 2018; Ghehi et al. 2012).

Thirthy seven out of 63 PTFs have used only the OC or OM content as a predictor to estimate BD, and the best-performant six PTFs, ranked according to the RMSE in Fig. 7, are based on OC or OM as a unique predictor. PTFs boost the information available for digital mapping, which can be utilized to develop indicators of soil quality, vulnerability and resilience. The uncertainty assessed in this study can be considered satisfactory in derived soil BD from primary soil properties such as topsoil OC or OM content and textural data.

Previous studies ranked the textural Cl, Si and Sa predictors differently. Al-Qinna and Jaber (2013) found that Sa and OC were the most crucial predictors for soil BD, while the effects of Cl and Si were not significant. Differently, Chen et al. (2018) proved that the Cl content was an important predictor, followed by Sa. Using empirical and ML models, Katuwal et al. (2020) found that Cl and OM contents significantly affected soil BD. Recently, Mishra et

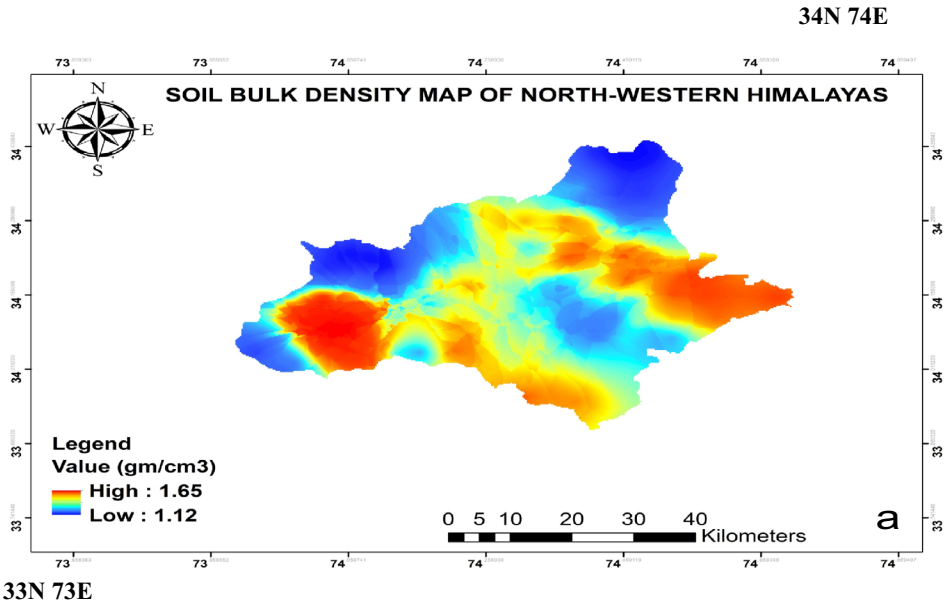

Fig. 8 Soil BD mapping of the study area

al. (2022) confirmed that the Cl content was the most important parameter related to soil BD. In this work, the correlation coefficient between Cl and BD was slightly positive but insignificant. In contrast, the correlation coefficient between Sa and BD was negative and statistically significant in explaining the variability of BD. Thus, this work explored the mathematical transformation of the original dependent variables by calibrating the MLR model.

The spatial soil BD map of the study area (Fig. 8) was developed using the PTF in Eq. 3 and Cl and OC maps as input variables. The BD maps provide an overview of sustainable agriculture management practices. These maps are instrumental for calculating vulnerability indicators and resilience to support the implementation of sustainable adaptation and mitigation strategies to restore degraded lands in the severely damaged NWH region described as the "snow-water erosion crisscross zone". In particular, the BD map shown in Fig. 8 can be considered an instrumental resource for immediately visualizing site-specific indicators, making them a powerful means for formulating appropriate mitigation and adaptation plans for soil conservation and land restoration. The BD map, combined with covariates, such as terrain features, land use and satellite images, can also be handy as a valuable input to construct process-oriented distributed eco-hydrological models.

4 Conclusions

In this study, the regression models PLSR, SR and LR, and the advanced ML algorithms ANN and DT were applied to develop a novel, intrinsically linear PTF for estimating soil BD based on soil textural and OC or OM data as predictors. Although ML methods are not constrained by linear assumptions and result in significantly improved predictive accuracy and more realistic representation of soil systems, they follow intricate patterns. On the other hand, the SR and PLSR methods, although they oversimplify complex nonlinear relationships, potentially leading to less accurate predictions, can be more advantageous than more advanced ones as they can operate on limited data sets and are easy to use and understand by researchers and stakeholder.

The novel stepwise regression-based PTF model (BD = 1.131 + 0.00299*Sa + 0.0051158*Cl-0.0388105*OC) enabled the evaluation of soil BD values (R^2, 0.73, RMSE, 0.0487 g cm^{-3}) in 300 soil samples representative of four land uses, i.e., agriculture, horticulture, forest and fallow, in the fragile hilly ecosystems of the NWH region. Furthermore, the SR-based PTF model developed in this work was shown to be more viable and accurate than the 63 PTFs available in the current literature (R^2 from 0.006 to 0.71, RMSE from 0.0649 to 0.405 g cm^{-3}) in predicting soil BD of the dataset. Differently from current models, the proposed realistic PTF model customized for the particular soils of the NWH region tackles regional issues and provides a dependable instrumentation for preservation and appropriate land management in hilly, erosion-prone areas. Furthermore, the PTF developed in this work features a broad potential for soil science and provides a starting point for future research studies to improve and broaden its use for effective land management. Future studies, however, should test advanced ML algorithms for PTF across various soil types and climates, while extending the dataset to include other varied hilly locations with additional predictor factors, including a wide range of soil properties, climate variables and additional land use patterns, in order to achieve a worldwide relevance in soil management and

digital mapping. Furthermore, advanced domain adoption methods and transfer learning can be expected to strengthen model performance across heterogenous conditions, so improving their generalization capabilities.

Although the availability of a new site-specific PTF offers a promising and efficient means to estimate soil BD with high precision and dependability, which implies essential practical aspects for land use planning and sustainability. This study explicitly acknowledges its limitation for any generalization due to its relatively limited dataset. Furthermore, since this PTF is site-specific to NWH, which is one of the most climatically unique regions, the PTF developed in this work cannot be directly scaled to different geographic and climatic regions. First of all, to address these limitations, a more diverse dataset encompassing different soil types, climates and land-use patterns is required. Additionally, integrating climate variables with feature selection methods and conducting external validation of the independent datasets, along with potential hybrid modeling approaches, are reasonably expected to improve the model robustness and transferability.

Authors Contributions Conceived and designed the study– Owais Bashir, Shabir Ahmad Bangroo, Shahid Shafai, Mario Palladino, Nicola Senesi, Burhan A Choudhary, Paolo Nasta and Shuraik Kader. Performed the analysis - Owais Bashir, Shabir Ahmad Bangroo, Sheikh Amjid, Paolo Nasta, Shahid Shafai, Mario Palladino, Nicola Senesi, Burhan A Choudhary, Prakash Kumar Jha, Rehana Rasool, Vikas Abrol, Velibor Spalevic, Paul Sestras, Negar Omidvar, Sezai Ercişli, Lizny Jaufer, Brahim Benzougagh, Youssef Bammou, Ksibi Mohamed, Tin Lukić, and Shuraik Kader. Data interpretation and validation - Owais Bashir, Shabir Ahmad Bangroo, Sheikh Amjid, Paolo Nasta, Shahid Shafai, Lizny Jaufer, Negar Omidvar, Sezai Ercişli, Mario Palladino, Nicola Senesi, Youssef Bammou, Tin Lukić, and Shuraik Kader. Contributed materials, analysis tools or data - Owais Bashir, Lizny Jaufer, Shabir Ahmad Bangroo, Sheikh Amjid, Rehana Rasool, Vikas Abrol, Youssef Bammou, and Shuraik Kader. Writing (original draft) - Owais Bashir, Shabir Ahmad Bangroo, Sheikh Amjid, Paolo Nasta, Shahid Shafai, Mario Palladino, Nicola Senesi, Burhan A Choudhary, Prakash Kumar Jha, Velibor Spalevic, Paul Sestras, Negar Omidvar, Sezai Ercişli, Lizny Jaufer, Brahim Benzougagh, Youssef Bammou, Ksibi Mohamed, Tin Lukić, and Shuraik Kader. Writing (reviewing and editing)– Brahim Benzougagh, Burhan A Choudhary, Mario Palladino, Nicola Senesi, Ksibi Mohamed, Paolo Nasta, Paul Sestras, Sezai Ercişli, and Velibor Spalevic. Project administration– Nicola Senesi, Owais Bashir, Paolo Nasta and Shuraik Kader. All authors have read and agreed to the submitted version of the manuscript.

Funding Open Access funding enabled and organized by CAUL and its Member Institutions
No fundings were received for this research.

Availability of data and materials The data and materials will be available on request.

Declaration

Conflict of interest The authors have no relevant financial or non-financial interests to disclose.

Open Access This article is licensed under a Creative Commons Attribution 4.0 International License, which permits use, sharing, adaptation, distribution and reproduction in any medium or format, as long as you give appropriate credit to the original author(s) and the source, provide a link to the Creative Commons licence, and indicate if changes were made. The images or other third party material in this article are included in the article's Creative Commons licence, unless indicated otherwise in a credit line to the material. If material is not included in the article's Creative Commons licence and your intended use is not permitted by statutory regulation or exceeds the permitted use, you will need to obtain permission directly from the copyright holder. To view a copy of this licence, visit http://creativecommons.org/licenses/by/4.0/.

References

Abdelbaki AM (2016) Using automatic calibration method for optimizing the performance of Pedotransfer functions of saturated hydraulic conductivity. Ain Shams Eng J 7(2):653–662. https://doi.org/10.1016/j.asej.2015.05.012

Abebe Ayalew B (2020) SOIL SURVEY AND FERTILITY ASSESSMENT OF ARGO-GEDILALA SUBWATERSHED IN DUGDA DISTRICT, CENTRAL RIFT VALLEY OF ETHIOPIA. Haramaya Univ. https://doi.org/10.5897/JLMA2021.0021

Adams W (1973) The effect of organic matter on the bulk and true densities of some uncultivated podzolic soils. J Soil Sci 24(1):10–17. https://doi.org/10.1111/j.1365-2389.1973.tb00737.x

Akpa S, Ugbaje S, Bishop T, Odeh I (2016) Enhancing Pedotransfer functions with environmental data for estimating bulk density and effective cation exchange capacity in a data-sparse situation. Soil Use Manag 32(4):644–658. https://doi.org/10.1111/sum.12310

Al-Qinna MI, Jaber SM (2013) Predicting soil bulk density using advanced Pedotransfer functions in an arid environment. Trans ASABE 56(3):963–976

Alexander E (1980) Bulk densities of California soils in relation to other soil properties. Soil Sci Soc Am J 44(4):689–692. https://doi.org/10.2136/sssaj1980.03615995004400040005x

Bansal S, Chakraborty P, Kumar S (2022) Crop–livestock integration enhanced soil aggregate-associated carbon and nitrogen, and phospholipid fatty acid. Sci Rep 12(1):1–13. https://doi.org/10.1038/s41598-022-06560-6

Bashir O, Bangroo SA, Guo W, Meraj G, Ayele T, Naikoo G, Taddese NB, H (2022) Simulating Spatiotemporal changes in land use and land cover of the North-Western Himalayan region using Markov chain analysis. Land 11(12):2276. https://doi.org/10.3390/land11122276

Bashir O, Bangroo SA, Shafai SS, Senesi N, Kader S, Alamri S (2024a) Geostatistical modeling approach for studying total soil nitrogen and phosphorus under various land uses of North-Western Himalayas. Ecol Inf 80:102520. https://doi.org/10.1016/j.ecoinf.2024.102520

Bashir O, Bangroo SA, Shafai SS, Senesi N, Naikoo NB, Kader S, Jaufer L (2024b) Unlocking the potential of soil potassium: Geostatistical approaches for Understanding Spatial variations in

Northwestern Himalayas. Ecol Inf 81:102592. https://doi.org/10.1016/j.ecoinf.2024.102592
Benites VM, Machado PL, Fidalgo EC, Coelho MR, Madari BE (2007) Pedotransfer functions for estimating soil bulk density from existing soil survey reports in Brazil. Geoderma 139(1–2):90–97. https://doi.org/10.1016/j.geoderma.2007.01.005
Bernoux M, Cerri C, Arrouays D, Jolivet C, Volkoff B (1998) Bulk densities of Brazilian Amazon soils related to other soil properties. Soil Sci Soc Am J 62(3):743–749. https://doi.org/10.2136/sssaj1998.03615995006200030029x
Beutler SJ, Pereira MG, Tassinari WdS, Menezes MDd, Valladares GS, Anjos LHCd (2017) Bulk density prediction for histosols and soil horizons with high organic matter content. Revista Brasileira De Ciência Do Solo 41. https://doi.org/10.1590/18069657rbcs20160158
Bossard M, Feranec J, Otahel J (2000) CORINE land cover technical guide: addendum 2000, vol 40. European Environment Agency Copenhagen
Botula Y-D, Nemes A, Van Ranst E, Mafuka P, De Pue J, Cornelis WM (2015) Hierarchical Pedotransfer functions to predict bulk density of highly weathered soils in central Africa. Soil Sci Soc Am J 79(2):476–486. https://doi.org/10.2136/sssaj2014.06.0238
Breusch TS, Pagan AR (1979) A simple test for heteroscedasticity and random coefficient variation. Econometrica: J Econometric Soc 1287–1294. https://doi.org/10.2307/1911963
Calhoun F, Smeck N, Slater B, Bigham J, Hall G (2001) Predicting bulk density of Ohio soils from morphology, genetic principles, and laboratory characterization data. Soil Sci Soc Am J 65(3):811–819. https://doi.org/10.2136/sssaj2001.653811x
Chen S, Richer-de-Forges AC, Saby NP, Martin MP, Walter C, Arrouays D (2018) Building a Pedotransfer function for soil bulk density on regional dataset and testing its validity over a larger area. Geoderma 312:52–63. https://doi.org/10.1016/j.geoderma.2017.10.009
Choudhury BU, Santra P, Singh N, Chakraborty P (2023) Development of land-use-specific Pedotransfer functions for predicting bulk density of acidic topsoil in Eastern Himalayas (India). Geoderma Reg 34:e00671. https://doi.org/10.1016/j.geodrs.2023.e00671
Cienciala E, Exnerova Z, Macku J, Henzlik V (2006) Forest topsoil organic carbon content in Southwest Bohemia region. J Sci (Prague) 52(9):387–398
Curtis RO, Post BW (1964) Estimating bulk density from organic-matter content in some Vermont forest soils. Soil Sci Soc Am J 28(2):285–286. https://doi.org/10.2136/sssaj1964.03615995002800020044x
Das L, Meher JK (2019) Drivers of climate over the Western Himalayan region of India: A review. Earth Sci Rev 198:102935. https://doi.org/10.1016/j.earscirev.2019.102935
De Vos B, Van Meirvenne M, Quataert P, Deckers J, Muys B (2005a) Predictive quality of Pedotransfer functions for estimating bulk density of forest soils. Soil Sci Soc Am J 69(2):500–510. https://doi.org/10.2136/sssaj2005.0500
De Vos M, Van Oosten VR, Van Poecke RM, Van Pelt JA, Pozo MJ, Mueller MJ, Dicke M (2005b) Signal signature and transcriptome changes of Arabidopsis during pathogen and insect attack. Mol Plant Microbe Interact 18(9):923–937. https://doi.org/10.1094/mpmi-18-0923
Dexter A (2004) Soil physical quality: part I. Theory, effects of soil texture, density, and organic matter, and effects on root growth. Geoderma 120(3–4):201–214. https://doi.org/10.1016/j.geoderma.2003.09.004
Drew LA (1973) Bulk density estimation based on organic matter content of some Minnesota soils
Eschner AR, Jones B, Moyle R (1957) Physical properties of 134 soils in six northeastern states. *Station Paper NE-89. Upper Darby, PA: US Department of Agriculture, Forest Service, Northeastern Forest Experiment Station. 11 p., 89*
Federer CA (1983) Nitrogen mineralization and nitrification: depth variation in four new England forest soils. Soil Sci Soc Am J 47(5):1008–1014. https://doi.org/10.2136/sssaj1983.03615995004700050034x
Federer C, Turcotte D, Smith C (1993) The organic fraction–bulk density relationship and the expression of nutrient content in forest soils. Can J for Res 23(6):1026–1032. https://doi.org/10.1139/x93-131
Gee GW, Or D (2002) 2.4 Particle-size analysis. Methods Soil Analysis: Part 4 Phys Methods 5:255–293. https://doi.org/10.2136/sssabookser5.4.c12
Ghehi NG, Nemes A, Verdoodt A, Van Ranst E, Cornelis W, Boeckx P (2012) Nonparametric techniques for predicting soil bulk density of tropical rainforest topsoils in Rwanda. Soil Sci Soc Am J 76(4):1172–1183. https://doi.org/10.2136/sssaj2011.0330
Grigal D, Brovold S, Nord W, Ohmann L (1989) Bulk density of surface soils and peat in the North central united States. Can J Soil Sci 69(4):895–900. https://doi.org/10.4141/cjss89-092
Hallet S, Hollis J, Keay C (1998) Derivation and evaluation of a set of pedogenically-based empirical algorithms for predicting bulk density in British soils. In: Citeseer
Han G-Z, Zhang G-L, Gong Z-T, Wang G-F (2012) Pedotransfer functions for estimating soil bulk density in China. Soil Sci 177(3):158–164. https://doi.org/10.1097/SS.0b013e31823fd493
Harrison A, Bocock K (1981) Estimation of soil bulk-density from loss-on-ignition values. J Appl Ecol 919–927. https://doi.org/10.2307/2402382
Hasan MM, Liu XD, Rahman MA et al (2025) Plants breathing under pressure: mechanistic insights into soil compaction-induced physiological, molecular and biochemical responses in plants. Planta 261:52. https://doi.org/10.1007/s00425-025-04624-1
Heuscher SA, Brandt CC, Jardine PM (2005) Using soil physical and chemical properties to estimate bulk density. Soil Sci Soc Am J 69(1):51–56. https://doi.org/10.2136/sssaj2005.0051a
Hijbeek R, Trombetti M, de Vries W, Baritz R (2019) An assessment of soil organic matter thresholds for crop production in Europe
Hollis J, Hannam J, Bellamy P (2012) Empirically-derived Pedotransfer functions for predicting bulk density in European soils. Eur J Soil Sci 63(1):96–109. https://doi.org/10.1111/j.1365-2389.2011.01412.x
Honeysett J, Ratkowsky D (1989) The use of ignition loss to estimate bulk density of forest soils. J Soil Sci 40(2):299–308
Hong SY, Minasny B, Han KH, Kim Y, Lee K (2013) Predicting and mapping soil available water capacity in Korea. PeerJ 1:e71. https://doi.org/10.7717/peerj.71
Hossain M, Chen W, Zhang Y (2015) Bulk density of mineral and organic soils in the Canada's Arctic and sub-arctic. Inform Process Agric 2(3–4):183–190. https://doi.org/10.1016/j.inpa.2015.09.001
Huntington T, Johnson C, Johnson A, Siccama T, Ryan D (1989) Carbon, organic matter, and bulk density relationships in a forested spodosol. Soil Sci 148(5):380–386
Hussen A, Munshi TA, Jahan LN, Hashan M (2024) Advanced machine learning approaches for predicting permeability in reservoir pay zones based on core analyses. Heliyon 10(12):e32666. https://doi.org/10.1016/j.heliyon.2024.e32666

Jeffrey D (1970) A note on the use of ignition loss as a means for the approximate Estimation of soil bulk density. J Ecol 297–299. https://doi.org/10.2307/2258183

Kanungo DP, Sharma S (2014) Rainfall thresholds for prediction of shallow landslides around Chamoli-Joshimath region, Garhwal Himalayas, India. Landslides 11(4):629–638. https://doi.org/10.1007/s10346-013-0438-9

Kaur R, Kumar S, Gurung H (2002) A pedo-transfer function (PTF) for estimating soil bulk density from basic soil data and its comparison with existing PTFs. Soil Res 40(5):847–858. https://doi.org/10.1071/SR01023

Keller T, Håkansson I (2010) Estimation of reference bulk density from soil particle size distribution and soil organic matter content. Geoderma 154(3–4):398–406. https://doi.org/10.1016/j.geoderma.2009.11.013

Kobal M, Urbančić M, Potočić N, De Vos B, Simončić P (2011) Pedotransfer functions for bulk density Estimation of forest soils. Šumarski List 135(1–2):19–27

Leonaviciute N (2000) Predicting soil bulk and particle densities by Pedotransfer functions from existing soil data in Lithuania. Geografijos Metraštis 33:7–330

Manrique L, Jones C (1991) Bulk density of soils in relation to soil physical and chemical properties. Soil Sci Soc Am J 55(2):476–481. https://doi.org/10.2136/sssaj1991.03615995005500020030x

Mebius LJ (1960) A rapid method for the determination of organic carbon in soil. Anal Chim Acta 22:120–124. https://doi.org/10.1016/S0003-2670(00)88254-9

Men M, Peng Z, Hao X, Yu Z (2008) Investigation on Pedotransfer function for estimating soil bulk density in Hebei Province. Chin J Soil Sci 1:20

Mengesha M, Tamiru S, CLASSIFICATION OF SALT AFFECTED SOILS OF AMBO-COBA AREA UNDER GOLINA WATERSHED IN RAYA KOBO VALLEY (2018) CHARACTERIZATION AND, AMHARA REGION, ETHIOPIA. Haramaya university

Minasny B, Hartemink AE (2011) Predicting soil properties in the tropics. Earth Sci Rev 106(1–2):52–62. https://doi.org/10.1016/j.earscirev.2011.01.005

Mourya KK, Barman A, Hota S, Tiwari G, Verma S, Kumar A, Saikia US (2024) Land degradation neutrality: concept and approaches. In: Regenerative Agriculture. CRC Press, pp. 71-93

Nanko K, Ugawa S, Hashimoto S, Imaya A, Kobayashi M, Sakai H, Takahashi M (2014) A Pedotransfer function for estimating bulk density of forest soil in Japan affected by volcanic Ash. Geoderma 213:36–45. https://doi.org/10.1016/j.geoderma.2013.07.025

Nasta P, Palladino M, Sica B, Pizzolante A, Trifuoggi M, Toscanesi M, Mazzitelli C (2020) Evaluating Pedotransfer functions for predicting soil bulk density using hierarchical mapping information in Campania, Italy. Geoderma Reg 21:e00267. https://doi.org/10.1016/j.geodrs.2020.e00267

Nazir S, uz Zaman Q, Al-Omran A, Hopmans JW, Ashraf K, Komal N, Baig MB (2022) Bioresource nutrient recycling and its relationship with soil health under irrigated Agro-ecosystems. In: Behnassi M, Gupta H, Barjees Baig M, Noorka IR (eds) The food security, biodiversity, and climate Nexus. Springer International Publishing, Cham, pp 441–477. https://doi.org/10.1007/978-3-031-12586-7_23

Noryani M, Sapuan SM, Mastura MT, Zuhri MYM, Zainudin ES (2019) Material selection of natural fibre using a Stepwise regression model with error analysis. J Mater Res Technol 8(3):2865–2879. https://doi.org/10.1016/j.jmrt.2019.02.019

Palladino M, Romano N, Pasolli E, Nasta P (2022) Developing Pedotransfer functions for predicting soil bulk density in campania. Geoderma 412:115726. https://doi.org/10.1016/j.geoderma.2022.115726

Perie C, Ouimet R (2008) Organic carbon, organic matter and bulk density relationships in boreal forest soils. Can J Soil Sci 88(3):315–325. https://doi.org/10.4141/CJSS06008

Popolizio S, Stellacci AM, Giglio L, Barca E, Spagnuolo M, Castellini M (2022) Seasonal and soil use dependent variability of physical and hydraulic properties: an assessment under minimum tillage and No-Tillage in a Long-Term experiment in Southern Italy. Agronomy 12(12):3142. https://doi.org/10.3390/agronomy12123142

Prévost M (2004) Predicting soil properties from organic matter content following mechanical site Preparation of forest soils. Soil Sci Soc Am J 68(3):943–949. https://doi.org/10.2136/sssaj2004.9430

Ramcharan AM (2017) Multidisciplinary applications of US soil datasets: machine learning models, data mining, and land use analyses. The Pennsylvania State University

Rawls W, Nemes A, Pachepsky Y (2004) Effect of soil organic carbon on soil hydraulic properties. Dev Soil Sci 30:95–114. https://doi.org/10.1016/S0166-2481(04)30006-1

Reidy B, Simo I, Sills P, Creamer RE (2016) Pedotransfer functions for Irish soils–estimation of bulk density (ρ b) per horizon type. Soil 2(1):25–39. https://doi.org/10.5194/soil-2-25-2016

Rodríguez-Lado L, Martínez-Cortizas A (2015) Modelling and mapping organic carbon content of topsoils in an Atlantic area of Southwestern Europe (Galicia, NW-Spain). Geoderma 245:65–73. https://doi.org/10.1016/j.geoderma.2015.01.015

Ruehlmann J, Körschens M (2009) Calculating the effect of soil organic matter concentration on soil bulk density. Soil Sci Soc Am J 73(3):876–885. https://doi.org/10.2136/sssaj2007.0149

Saini G (1966) Organic matter as a measure of bulk density of soil. Nature 210(5042):1295–1296. https://doi.org/10.1038/2101295a0

Schillaci C, Saia S, Lipani A, Perego A, Zaccone C, Acutis M (2021) Validating the regional estimates of changes in soil organic carbon by using the data from paired-sites: The case study of Mediterranean arable lands. Carbon Balance Manage 16(1):19. https://doi.org/10.1186/s13021-021-00182-7

Sequeira AM, Roetman PE, Daniels CB, Baker AK, Bradshaw CJ (2014) Distribution models for Koalas in S outh A Ustralia using citizen science-collected data. Ecol Evol 4(11):2103–2114. https://doi.org/10.1002/ece3.1094

Sevastas S, Gasparatos D, Botsis D, Siarkos I, Diamantaras KI, Bilas G (2018) Predicting bulk density using Pedotransfer functions for soils in the upper Anthemountas basin, Greece. Geoderma Reg 14:e00169. https://doi.org/10.1016/j.GEODRS.2018.e00169

Sharma A, Jain A, Gupta P, Chowdary V (2020) Machine learning applications for precision agriculture: A comprehensive review. IEEE Access 9:4843–4873. https://doi.org/10.1109/ACCESS.2020.3048415

Sharma A, Patel SK, Barla A et al (2024) Evaluating variability in soil attributes and forest vegetation in a degraded dry tropical region: an ecological restoration perspective. Environ Dev Sustain. https://doi.org/10.1007/s10668-024-05811-y2

Shiri J, Keshavarzi A, Kisi O, Karimi S, Iturraran-Viveros U (2017) Modeling soil bulk density through a complete data scanning procedure: heuristic alternatives. J Hydrol 549:592–602. https://doi.org/10.1016/j.jhydrol.2017.04.035

Song G, Li L, Pan G, Zhang Q (2005) Topsoil organic carbon storage of China and its loss by cultivation. Biogeochemistry 74(1):47–62. https://doi.org/10.1007/s10533-004-2222-3

Svoray T (2022) Soil erosion: the general problem. In: Svoray T (ed) A geoinformatics approach to water erosion: soil loss and beyond. Springer International Publishing, Cham, pp 1–38. https://doi.org/10.1007/978-3-030-91536-0_1

Tamminen P, Starr M (1994) Bulk density of forested mineral soils

Tomasella J, Hodnett MG (1998) Estimating soil water retention characteristics from limited data in Brazilian Amazonia. Soil Sci 163(3):190–202

Tranter G, Minasny B, McBratney A, Murphy B, McKenzie N, Grundy M, Brough D (2007) Building and testing conceptual and empirical models for predicting soil bulk density. Soil Use Manag 23(4):437–443. https://doi.org/10.1111/j.1475-2743.2007.00092.x

Tremblay S, Ouimet R, Houle D (2002) Prediction of organic carbon content in upland forest soils of Quebec, Canada. Can J for Res 32(5):903–914. https://doi.org/10.1139/x02-023

Valzano F, Murphy B, Koen T (2005) national carbon accounting system. In: Canberra, Australia: Australian Greenhouse Office. Technical Report

Williams R (1971) Relationships between the composition of soils and physical measurements made on them. Rothamsted Experimental Stn Rep 1970Part 2:5–35. https://doi.org/10.23637/ERADOC-1-34799

Wu H, Guo Z, Peng C (2003) Land use induced changes of organic carbon storage in soils of China. Glob Change Biol 9(3):305–315. https://doi.org/10.1046/j.1365-2486.2003.00590.x

Xiangsheng Y, Guosheng L, Yanyu Y (2016) Pedotransfer functions for estimating soil bulk density: A case study in the Three-River headwater region of Qinghai Province, China. Pedosphere 26(3):362–373. https://doi.org/10.1016/S1002-0160(15)60049-2

Yang Y, Mohammat A, Feng J, Zhou R, Fang J (2007) Storage, patterns and environmental controls of soil organic carbon in China. Biogeochemistry 84(2):131–141. https://doi.org/10.1007/s10533-007-9109-z

Zinke PJ, Millemann RE, Boden TA (1986) Worldwide organic soil carbon and nitrogen data. Carbon Dioxide Information Center, Environmental Sciences Division, Oak Ridge National Laboratory

Publisher's Note Springer Nature remains neutral with regard to jurisdictional claims in published maps and institutional affiliations.

Authors and Affiliations

Owais Bashir[1] · Shabir Ahmad Bangroo[1] · Sheikh Amjid[1] · Paolo Nasta[2] · Shahid Shafai[1] · Mario Palladino[2] · Nicola Senesi[3] · Rehana Rasool[1] · Burhan A. Choudhary[4] · Prakash Kumar Jha[5] · Vikas Abrol[6] · Velibor Spalevic[7] · Paul Sestras[8,9] · Negar Omidvar[10] · Sezai Ercişli[11] · Lizny Jaufer[12] · Brahim Benzougagh[13] · Youssef Bammou[14] · Ksibi Mohamed[15] · Tin Lukić[16] · Shuraik Kader[17]

✉ Shuraik Kader
s.mohamedabdulkader@griffith.edu.au

Owais Bashir
owaisbashir10@skuastkashmir.ac.in

Shabir Ahmad Bangroo
shabir@skuastkashmir.ac.in

Sheikh Amjid
amjidsheikh66@gmail.com

Paolo Nasta
paolo.nasta@unina.it

Shahid Shafai
shahidshafai@gmail.com

Mario Palladino
mpalladi@unina.it

Nicola Senesi
nicola.senesi@uniba.it

Rehana Rasool
rasoolroohi@yahoo.co.in

Burhan U. Choudhury
burhan.icar@gmail.com

Prakash Kumar Jha
pj442@msstate.edu

Vikas Abrol
abrolvics@gmail.com

Velibor Spalevic
velibor.spalevic@gmail.com

Paul Sestras
paul.sestras@usamvcluj.ro; psestras@yahoo.com

Negar Omidvar
n.omidvar@griffith.edu.au

Sezai Ercişli
sercisli@atauni.edu.tr; sercisli@gmail.com

Lizny Jaufer
lizny96@gmail.com

Brahim Benzougagh
brahim.benzougagh@is.um5.ac.ma

Youssef Bammou
youssef.bammou@ced.uca.ma

Ksibi Mohamed
mdh.ksibi@gmail.com; mohamed.ksibi@isbs.usf.tn

Tin Lukić
tin.lukic@dgt.uns.ac.rs

[1] Division of Soil Science, Sher-e-Kashmir University of Agricultural Sciences and Technology of Kashmir, Srinagar, Jammu and Kashmir 190025, India

[2] Department of Agricultural Sciences, AFBE Division, University of Naples Federico II, Portici (Naples, Italy

[3] Department of Soil, Plant and Food Sciences, University of Bari Aldo Moro, Bari, Italy

[4] Division of NRM, ICAR Research Complex for NEH Region, Umiam 793103, Meghalaya, India

[5] Agricultural Climatology Department of Plant and Soil Sciences, Mississippi State University, 225 Dorman Hall, 32 Creelman Street, Starkville, Mississippi State, MS 39762, USA

[6] Division of Soil Science, Sher-e-Kashmir University of Agricultural Sciences and Technology of Jammu, , Srinagar 181102, Jammu and Kashmir, India

[7] Biotechnical Faculty, University of Montenegro, Podgorica 81000, Montenegro

[8] Faculty of Forestry and Cadastre, University of Agricultural Sciences and Veterinary Medicine Cluj-Napoca, Cluj-Napoca 400372, Romania

[9] Academy of Romanian Scientists, Ilfov 3, Bucharest 050044, Romania

[10] Centre for Planetary Health and Food Security, Griffith University, Brisbane 4111, QLD, Australia

[11] Faculty of Agriculture, Department of Horticulture, Ataturk University, 25240 Erzurum, Turkey

[12] Machine Minds Academy, 12 Wulfstan Way, CB18QH Cambridge, UK

[13] Geophysics and Natural Hazards Laboratory, Department of Geomorphology and Geomatics (D2G), Scientific Institute, Mohammed V University in Rabat, Avenue Ibn Batouta, PO Box 703, Agdal, Rabat- City 10106, Morocco

[14] Laboratory of Geo-Resources, Department of Geology, Faculty of Science and Technology, Geo-Environment and Civil Engineering (L3G), Cadi Ayyad University, Marrakesh, Morocco

[15] Laboratory of Environmental Engineering and Ecotechnology, National School of Engineers of Sfax (ENIS), University of Sfax, Route de Soukra Km 3.5, Po. Box 1175, Sfax 3038, Tunisia

[16] Department of Geography, Tourism and Hotel Management, Faculty of Sciences, University of Novi Sad, Trg Dositeja Obradovića 3, Novi Sad 21000, Serbia

[17] School of Engineering and Built Environment, Griffith University, Nathan, QLD 4111, Australia